Available online at www.sciencedirect.com
ScienceDirect

Journal of Photochemistry and Photobiology A: Chemistry 194 (2008) 344–350

Journal of Photochemistry and Photobiology A:Chemistry

www.elsevier.com/locate/jphotochem

A novel two-stage process for laser enrichment of sulphur isotopes

P. Mathi [a], P.K. Sahoo [a], D.N. Joshi [a], M.N. Deo [b], A.K. Nayak [a],
S.K. Sarkar [c], V. Parthasarathy [a,*]

[a] *Laser & Plasma Technology Division, Bhabha Atomic Research Centre, Mumbai 400085, India*
[b] *High Pressure Physics Division, Bhabha Atomic Research Centre, Mumbai 400085, India*
[c] *Radiation & Photochemistry Division, Bhabha Atomic Research Centre, Mumbai 400085, India*

Received 10 May 2007; received in revised form 29 August 2007; accepted 31 August 2007
Available online 11 September 2007

Abstract

A novel two-stage approach is invoked for the laser enrichment of sulphur isotopes. It consists of sequentially photolysing SF_6 at −78 °C in the same cell with different lines of the CO_2 laser in different stages. The requisite chemical link between the stages is facilitated by carefully controlling the presence or absence of a scavenger during irradiation. Our results show that enrichment of S-33 is viable by such an approach.

Keywords: Sulphur-33; Laser enrichment; IR MPD

1. Introduction

Sulphur has four stable isotopes with the following natural abundance:

$$\%{}^{32}S : {}^{33}S : {}^{34}S : {}^{36}S = 95.0 : 0.76 : 4.22 : 0.014$$

Sulphur-33 (S-33) is required as a target material for producing phosphorous-33 (P-33) in the nuclear reactor using the reaction ${}^{33}S(n,p){}^{33}P$. Phosphorous-33 has, of late, emerged as an important radioisotope for molecular biology and life science research due to its special radiation characteristics vis-à-vis those of P-32 and S-35 [1,2] (Table 1). The present work deals with the feasibility of such an enrichment process by infrared laser chemistry of SF_6. Studies on isotopically selective, infrared multiphoton dissociation (IRMPD) of SF_6 have been well documented in the literature [3–10]. While most of the works were aimed at enrichment of S-32 or S-34 isotopes, a few attempted to enrich S-33 [5,9,10].

The ν_3 absorption features of the two prominent isotopic variants ${}^{32}SF_6$ (95%) and ${}^{34}SF_6$ (4.2%) are separated by an isotope shift of 17 cm^{-1} [11]. Various isotopic species, in principle, can be selectively excited and dissociated by the appropriate frequency of the CO_2 laser emitting in 10.3 μm band (cf. Fig. 1). The isotope shift between the adjacent pair of isotopic species have been calculated to be 8.5 cm^{-1} [11]. There is a considerable overlap between the absorption bands of these species and the spectral features are not clearly resolved at room temperature. Previous attempts to enrich S-33 by direct excitation of ${}^{33}SF_6$ in a single stage were not successful [9]. In all the enrichment runs by IR MPD, the major species ${}^{32}SF_6$ was selectively excited and dissociated in natural SF_6 sample and the residual material became enriched in S-33 and S-34 species [3–10]. Therefore, for a high degree of enrichment in S-33, a two-stage process would be required:

- *Stage 1.* In stage 1, ${}^{32}SF_6$ is targeted and dissociated selectively using a pulsed CO_2-laser tuned at appropriate wavelength and the product formed is removed.

  $${}^{32}SF_6 \rightarrow {}^{32}SF_5 + F \rightarrow {}^{32}SF_4 + F \rightarrow \text{products}$$

  The residual SF_6 material recovered will be enriched in S-34 and S-33 isotopes compared to the initial natural abundance levels.
- *Stage 2.* In stage 2 of the process, ${}^{34}SF_6$ may be selectively dissociated so that the residual SF_6 is further enriched in S-33 isotope compared to that in stage 1.

  $${}^{34}SF_6 \rightarrow {}^{34}SF_5 + F \rightarrow {}^{34}SF_4 + F \rightarrow \text{products}$$

---

[*] Corresponding author.
E-mail address: partha@barc.gov.in (V. Parthasarathy).

1010-6030/$ – see front matter © 2007 Elsevier B.V. All rights reserved.
doi:10.1016/j.jphotochem.2007.08.034

Table 1
Properties of radioactive nuclei

Radioisotope	Formation in the nuclear reaction	Half-life (days)	Nuclear decay reaction	Maximum energy of β emitted (MeV)
Phosphorous-32	^{32}S(n,p)^{32}P	14.3	^{32}P(-β)^{32}S	1.71
Phosphorous-33	^{33}S(n,p)^{33}P	25.4	^{33}P(-β)^{33}S	0.249
Sulphur-35	^{34}S(n,γ)^{35}S	87.4	^{35}S(-β)^{35}Cl	0.167

It has been shown that IR laser chemistry of SF_6 leads to an array of products [3–9] through various secondary steps:

$$SF_6 \rightarrow SF_5 + F(\text{primary photodissociation}) \quad (1)$$

$$SF_5 \rightarrow SF_4 + F(\text{secondary photodissociation}) \quad (2)$$

$$SF_5 + F \rightarrow SF_6(\text{recombination}) \quad (3)$$

$$SF_5 + SF_5 \rightarrow S_2F_{10} \rightarrow SF_4 + SF_6(\text{dis-proportionation}) \quad (4)$$

It is necessary to prevent processes like (3) and (4) as they regenerate SF_6. It is also essential to trap SF_5 which undergoes dimerisation to S_2F_{10}. The latter species is responsible for the dis-proportionation reaction (4) which regenerates SF_6. Such reactions are detrimental to the enrichment scheme as they lead to poor decomposition efficiency.

Fuss and Schmidt [12] have used a mixture of BaO/triethyleneglycol (Trigol) while Baranov et al. [5] have used BaO/triethanolamine mixture for scavenging SF_4 and HF based on the following chemical steps:

$$SF_4 + 3BaO \rightarrow 2BaF_2 + BaSO_3 \quad (5)$$

$$2HF + BaO \rightarrow BaF_2 + H_2O \quad (6)$$

$$H_2O + BaO \rightarrow Ba(OH)_2 \quad (7)$$

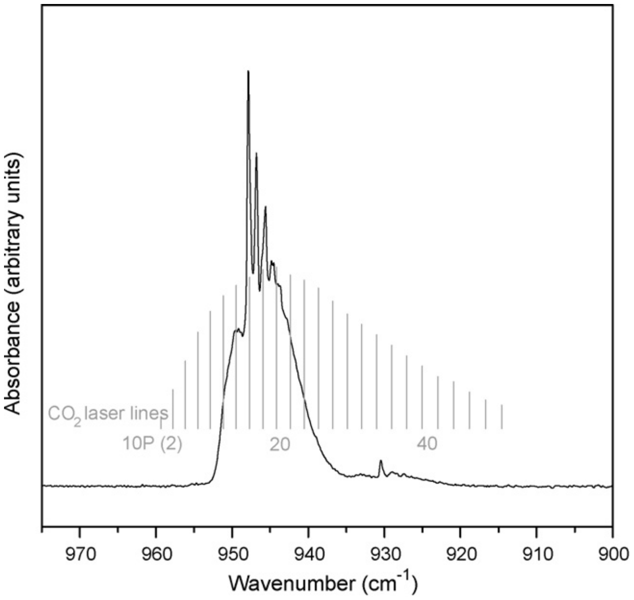

Fig. 1. Absorption spectrum of natural SF_6 recorded at a resolution of 0.2 cm^{-1} CO_2 laser lines superimposed on SF_6 spectrum.

Besides reactions (1)–(4), irradiation also produced a number of species such as SOF_2, SO_2F_2, SiF_4 which were identified by their characteristic IR features. The formation of these species could be attributed to the secondary reactions of SF_5 and SF_4 with moisture adsorbed on the cell surface. In the present paper, we have first examined the possibility of using various reactive gases such as H_2, O_2 and Cl_2 as scavengers. The idea was two fold, viz., (i) to investigate the efficacy of these species in trapping the primary photoproducts, viz., SF_5 and F radicals and (ii) whether we can obtain a useful stage 1 end product which will help in closing the chemical cycle for stage 2.

We have also tried using a mixture of NaOH/triethyleneglycol (Trigol) during the photolysis of neat SF_6 and checked its effectiveness in trapping a number of primary and secondary photoproducts.

Further by cooling the substrate gas during photolysis, rotational structure effects and hot bands absorption can be minimized to improve upon the process selectivity [5,9]. Therefore, IR MPD of natural SF_6 was carried out at dry ice temperature (−78 °C) in order to enrich the S-33 considerably.

In IR laser chemistry, it has been demonstrated [13,14] that a two-stage process is more beneficial than a single stage process to achieve very high isotopic enrichment levels (>90%). However, closing the chemical cycle between the two stages is a non-trivial issue. Sometimes starting material for stage 2 photolysis is obtained from stage 1, physically separated and employed in stage 2 [13]. In some fortuitous cases, the intermediate product obtained undergoes in situ photolysis absorbing laser radiation at the same frequency as that of the starting material and produces the end product highly enriched with the targeted minor isotope [14]. In the present context, we have adapted a novel two-stage approach. It consists of sequentially executing the photolysis process in the same cell in situ with different lines in different stages. The requisite chemical link between the stages is facilitated by carefully controlling the presence or absence of scavenger during the irradiation. Our results indeed show that S-33 enrichment is realizable by such an approach.

2. Experimental

Photolysis with the 10 P(20) line of a 10 W pulsed CO_2 laser (Macro Optica) was carried out with neat SF_6 as well as SF_6/scavenger mixture using tail-free, 100 ns FWHM pulses at room temperature. The pulse energy was typically about 1.5 J and was focused by a BaF_2 lens (f = 75 cm) into the centre of a cylindrical Pyrex cell (length: 50 cm, volume: 467 cm^3) which had provision for IR analysis. Before and after photolysis, $^{32}SF_6$ absorption was measured at 947.359 cm^{-1} for pressures lower than 0.5 Torr of SF_6 and at 949.288 cm^{-1} for higher pressures while $^{34}SF_6$ absorption was monitored at 930.244 cm^{-1} by infrared spectrophotometry (Jasco 460 Plus and Bomem DA8). The uncertainty in these measurements is ±1%. From the extent of decomposition in each species after a certain number of pulses, the specific decomposition rate $d(x)$, can be obtained using the expression:

$$d(x) = 1 - \left(\frac{N(x)}{N_0(x)}\right)^{1/n}; \quad x = {}^{32}SF_6 \text{ or } {}^{34}SF_6 \tag{8}$$

where $N_0(x)$ and $N(x)$ represent the number of a particular isotopic species initially and after "n" pulses of irradiation.

When the laser is selectively tuned to excite and decompose $^{32}SF_6$ species in natural SF_6 sample, residual SF_6 becomes progressively depleted in $^{32}SF_6$ and gets enriched in $^{34}SF_6$ and $^{33}SF_6$. From the measured specific decomposition rates for each isotopic species, dissociation selectivity, S, in a typical run is obtained as the ratio:

$$S = \frac{d(^{32}SF_6)}{d(^{34}SF_6)} \tag{9}$$

The residual enrichment factor, β_{34}, for S-34 isotope with respect to S-32 is calculated from the equation:

$$\beta_{34} = \frac{(^{34}SF_6/^{32}SF_6)_{\text{after photolysis}}}{(^{34}SF_6/^{32}SF_6)_{\text{before photolysis}}} \tag{10}$$

In the preliminary studies, a U-trap containing NaOH pellets suspended in Trigol was attached to the photolysis cell as a side arm. Subsequently, a scavenger trap with provision for stirring the NaOH/Trigol slurry kept in a 250 cm^3 flat bottom flask was used. The detachable trap was directly mounted to the cell body at a distance of ∼42 cm from the cell entrance. The larger photolysis cell had an overall volume of 1505 cm^3 with an irradiation path length of 64 cm. This trap design was found to be superior to the U-trap used in the earlier investigations.

For low temperature experiments, a stainless steel cell (73 cm long; volume 231 cm^3) was designed and fabricated with provision for IR analysis. The cell was kept in a wooden box and packed with dry ice with proper thermal insulation. The entire assembly was aligned with the CO_2 laser using a He–Ne laser. Photolysis of natural SF_6 at ∼0.3 Torr was done by 10 P(18) line in stage 1 and the residual, enriched sample was further irradiated in the same cell in stage 2 at appropriate laser frequency with 100 ns tail-free pulses. Another important modification incorporated in the metallic cell was the provision of an isolation valve between the cell and the scavenger trap. This feature was very useful in controlling the exposure of the photolysed material to scavenger during the run as and when required. In the first stage, for example, all the photoproducts like SOF_2/SO_2F_2 were allowed to react with NaOH/Trigol scavenger during the run and the end product was only residual enriched SF_6. In the second stage photolysis, access to the scavenger was turned off and the laser was selectively tuned $^{33}SF_6$ excitation/dissociation resulting in direct enrichment of S-33 in the photoproduct, viz., SO_2F_2.

3. Results and discussion

3.1. Stage 1 photolysis studies at room temperature

For any LIS scheme, parametric variation studies are essential to fix the optimum experimental conditions for maximizing the dissociation selectivity, S and enrichment factor, β for a desired isotope. Generally the data base for S and β are generated as a function of energy fluence, substrate pressure, pulse duration and focusing geometry. When the minor isotopes S-33 and S-34 get enriched in residual material by the selective targeting of the major isotope S-32, both S and β strongly depend on the conversion extent. Therefore, the (N/N_0) ratio was measured in all the parametric studies as a function of the number of pulses in each experimental run for both S-32 and S-34 species. From the slopes of semi-log plots of (N/N_0) versus number of pulses, average specific decomposition rates $d(^{32}SF_6)$ and $d(^{34}SF_6)$ during the run were obtained (cf. Fig. 2 for a set of typical plots at different SF_6 pressures). These "d" values were used to estimate the S and β values using Eqs. (9) and (10), respectively. The overall uncertainty in S values given in Table 2 is estimated to be ±5%. The results follow the general trend reported in the literature [3–10] that photolysis of natural SF_6 at ∼0.3 Torr with 10 P(20) line by tail-free pulses at ∼6 J cm^{-2} resulted in more favorable decomposition of $^{32}SF_6$ compared to that for $^{34}SF_6$. At higher pressures or in the presence of any scavenger, the $^{32}SF_6$ decomposition extent was found to decrease due to collisional processes. Such processes also led to lower values for the dissociation selectivity. The frequency variation studies on neat SF_6 photolysis showed that $^{32}SF_6$ burning was relatively higher for irradiation with 10 P(18) line compared to those obtained for 10 P(20) and 10 P(16) lines.

Our studies on the suitability of various reactive gases such as H_2, O_2 and Cl_2 as scavengers gave some additional interesting results. While the species like H_2, O_2 and Cl_2 were effective in trapping SF_5 and F, many new volatile by-products

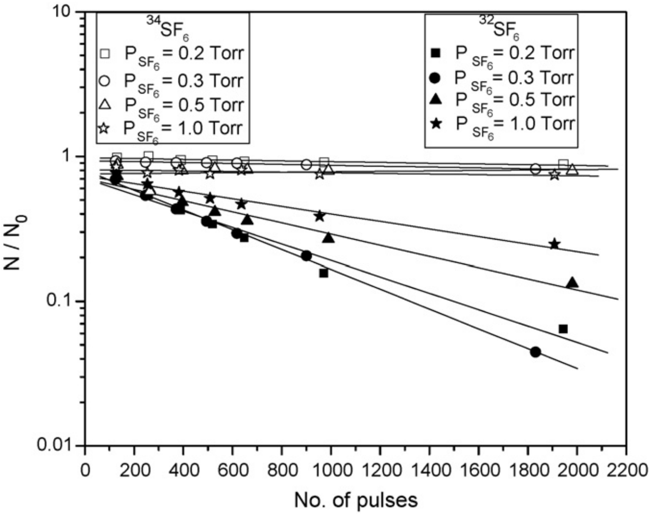

Fig. 2. Semi-log plot of (N/N_0) vs. number of pulses for neat SF_6 (room temperature) photolysis at different pressures. Fluence = 6 J/cm^2 and laser line = 10 P(20).

Table 2
SF_6 IR MPD parametric studies at room temperature

Details of parametric studies	Experimental condition	Dissociation selectivity, S
Pressure variation (neat SF_6, 10 P(20), 100 ns pulses, $\varphi = 7.0\,J\,cm^{-2}$)	0.2 Torr	21
	0.3 Torr	22
	0.5 Torr	15
	1.0 Torr	12
Fluence variation (10 P(20), 100 ns pulses, 0.3 Torr, $f = 75$ cm)	$\varphi = 5.0\,J\,cm^{-2}$	12
	$\varphi = 6.3\,J\,cm^{-2}$	18
	$\varphi = 7.0\,J\,cm^{-2}$	22
	$\varphi = 7.5\,J\,cm^{-2}$	15
Focusing geometry variation ((f: lens focal length), 10 P(20), 100 ns pulses, 0.3 Torr)	$f = 50$ cm	87
	$f = 75$ cm	23
	$f = 100$ cm	13

Details of parametric studies	Scavenger	Dissociation selectivity, S
SF_6–scavenger studies (total pressure for 1:5 mixture: 1.8 Torr)	Nil (neat SF_6: 0.3 Torr)	23
	H_2	16
	O_2	10
	Cl_2	21
SF_6/NaOH system	NaOH (SF_6: 0.3 Torr)	11
SF_6/NaOH/Trigol system	NaOH/Trigol (SF_6: 0.3 Torr)	19

were observed from the IR spectra taken after photolysis. These included SOF_2 (hydrolysis product from SF_4 with traces of moisture), SO_2F_2, S_2F_{10}, SF_5Cl and SiF_4. SiF_4 formation was traced to the attack on SiO_2 present in pyrex glass by F atoms. Therefore, physical isolation process for the residual SF_6 enriched in S-33 and S-34 species for subsequent use in stage 2 became more difficult. Also, some of these products were found to have spectral interference with the bands of measurement especially near $^{34}SF_6$ absorption. All these problems could be circumvented by the use of NaOH/Trigol mixture for scavenging SF_5/SF_4 and other secondary products which provided cleaner, residual SF_6 enriched in S-33 and S-34 isotopes free from any other volatile products.

In three separate batches, 0.3 Torr SF_6 was irradiated in the 467 cm^3 cell with built-in NaOH/Trigol trap and more than 90% of $^{32}SF_6$ was burnt and residual SF_6 samples from three batches of irradiation with 10 P(20) line were collected together and the FTIR spectrum (cf. Fig. 3) of the combined material was recorded at 0.2 cm^{-1} resolution. The relative abundance of $^{32}SF_6$:$^{33}SF_6$:$^{34}SF_6$ of this enriched sample was estimated to be 20:10:70%.

3.2. Stage 2 photolysis studies at room temperature

Stage 1 photolysis was done in several batches in order to collect a sizeable quantity of residual SF_6 enriched in S-33 and S-34 for subsequent use in stage 2. But the repeated cryogenic transfer operations of very small quantities of gases resulted in collecting appreciable quantity of moisture along with the enriched material. Our purification attempts were not successful. Therefore, both first and second stages of the enrichment process were attempted in a single batch using the same cell without involving any material transfer process under cryogenic conditions. For the stage 1 process, 0.3 Torr of natural SF_6 was photolysed by 10 P(18) line in the Pyrex cell with 16,700 pulses. At the end, the residual sample had an isotopic composition of 11:8:81% for ^{32}S:^{33}S:^{34}S, respectively. There was a loss of ~50% in the inventory of $^{33}SF_6$ at the end of stage 1 photolysis. In order to target the S-34 species in stage 2, laser was tuned to 10 P(38) line. After 21,500 shots, final composition was found to be 20:14:66, respectively, for ^{32}S:^{33}S:^{34}S. Apparently the stage 2 process of selective burning of $^{34}SF_6$ was not quite successful as the average pulse energy obtained for the weak 10 P(38) line was only 0.3 J as against 1.1 J for 10 P(18) line.

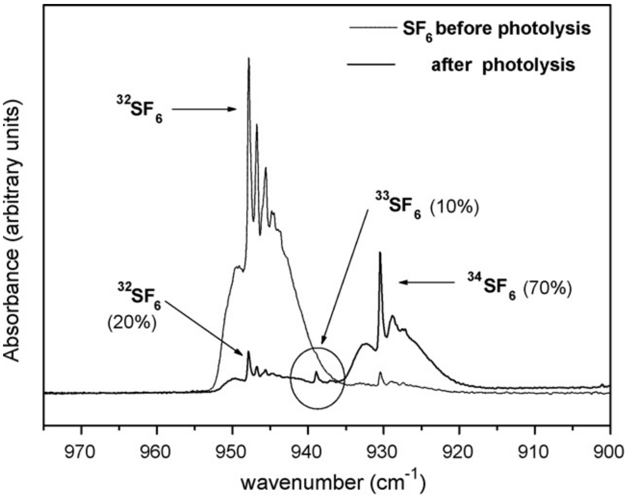

Fig. 3. Absorption spectrum of natural SF_6 (thin line) and enriched SF_6 (solid line). Three batches irradiated at room temperature. Pressure = 0.3 Torr, laser line: 10 P(18), fluence = 6 J/cm^2.

Table 3
Summary of photolysis runs at −78 °C

Serial no.	Stage 1 (laser line, pulse energy)	Pressure (scavenger)	Stage 2 (laser line, pulse energy)	% Composition (overall) ^{32}S:^{33}S:^{34}S (residual SF_6)
1	10 P(18), 1.2 J	0.29 Torr (Nil)	Not done	~0:~0:100
2	10 P(18), 1.1 J	0.34 Torr (Nil)	Not done	~0:14:86
3	10 P(18), 1.1 J	0.6 Torr (NaOH + trigol in 250 cm^3 bulb)	Not done	~0:14:86
4	10 P(18), 1.1 J	0.5 Torr (Nil)	10 P(38) 0.2 J	6:16:78
5	10 P(18), 1.3 J	0.44 Torr (Nil)	10 P(38) 0.6 J	33:12:55
6	10 P(18), 1.1 J	0.41 Torr (Nil)	10 P(26) 1.0 J	~0:~0:100
7	10 P(18), 1.2 J	0.42 Torr (NaOH + trigol in 250 cm^3 bulb)	10 P(26) 1.2 J (scavenger isolated)	~0:~0:100 (after stage 2)

3.3. Photolysis studies at low temperature

Molecular vibrational transitions spread out over a large range owing to the rotational structure and hot bands [15]. In fact, for heavier elements, the overlap is so serious that the isotope shift is not resolved at room temperature. Even for light and middle mass elements like Sulphur, it can lead to poor selectivity for both excitation and dissociation steps. Such rotational structure and hot bands absorption can be minimized to obtain better process selectivity by cooling the substrate gas during photolysis. Therefore, we investigated the IR MPD of natural SF_6 at dry ice temperature (−78 °C). The experimental details and results obtained are summarized in Table 3.

From these results, the following conclusions could be drawn. The appreciable loss seen in the desired isotopic species, viz., $^{33}SF_6$ when photolysis was done at room temperature can be minimized by working at low temperature which gave rise to better dissociation selectivity. Our efforts to obtain a final residual SF_6 highly enriched in $^{33}SF_6$ were not successful as we ended up burning it completely during stage 2 removal of $^{34}SF_6$. Fig. 4 for example shows the spectrum obtained for a residual SF_6 highly enriched in S-34. From this important observation we realized that it would be advantageous to selectively dissociate $^{33}SF_6$ in stage 2 rather than the removal of $^{34}SF_6$. Such an approach has two advantages, viz., (i) the inherent loss of S-33 associated with the excitation of $^{34}SF_6$ using a red-shifted absorption frequency will be absent (ii) the line 10 P(26) required for $^{33}SF_6$ dissociation has better laser efficiency than 10 P(38) used for $^{34}SF_6$ removal.

The above idea can be conveniently accomplished by carefully controlling the exposure of irradiated material to the scavenger in different stages of photolysis. The aim of carrying out the runs with and without scavenger, respectively, in stages 1 and 2 is twofold. In stage 1, when the S-32 species is selectively burnt, photoproduct, SO_2F_2 (predominantly enriched in S-32) needs to be trapped by the scavenger leaving only the residual SF_6 (enriched in S-33 and S-34 species) in the gas phase.

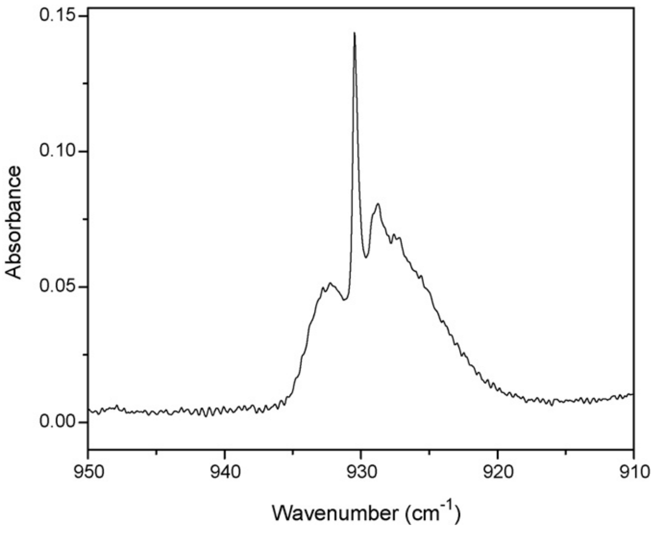

Fig. 4. Spectral feature of highly enriched $^{34}SF_6$.

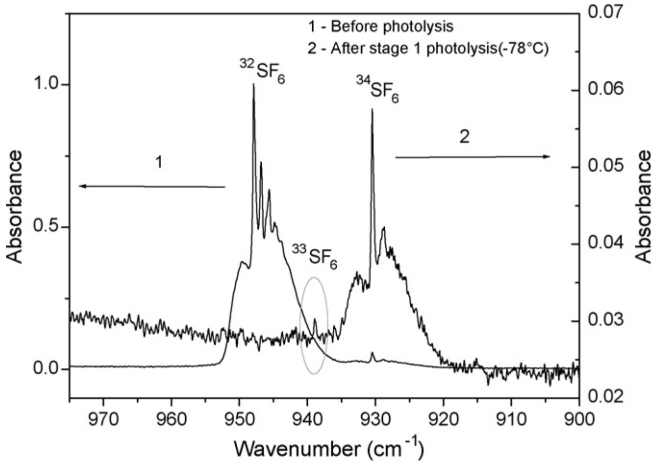

Fig. 5. Natural SF_6 before photolysis (^{32}S:^{33}S:^{34}S = 95:0.76:4.22). Enriched SF_6 after stage 1 photolysis at −78 °C (^{32}S:^{33}S:^{34}S = ∼0:12:88).

However, during stage 2 photolysis in the same cell, scavenger trap has to be kept isolated so that formation of the end product SO_2F_2 (enriched in S-33) is facilitated.

In one such run (cf. Run #7 in Table 3 for details), ∼99.6% of initial $^{32}SF_6$ was selectively burnt in the presence of scavenger (cf. Fig. 5). When this material was further irradiated in situ using 10 P(26) line in the absence of scavenger, ∼39% of $^{33}SF_6$ was found to be decomposed while there was no measurable dissociation in $^{34}SF_6$ after 900 shots (≤1%). Fig. 6 represents the overlay spectra of a single batch of sample before and after stage 2 photolysis in the 975–900 cm^{-1} region to demonstrate the disappearance of $^{33}SF_6$ band. Our efforts to look for the signatures of S-33 enriched SO_2F_2 and SOF_2 products by their characteristic IR bands reported in the literature [16] were not quite successful as these products' quantity was not enough to get a good S/N ratio. However, Figs. 7 and 8 qualitatively highlight the difference in IR spectral features in the SF_2 asymmetric stretching region of SO_2F_2 depending on the selective excitation/dissociation of $^{32}SF_6$ or $^{33}SF_6$. It would have been ideal to measure the individual isotopic composition in SO_2F_2 for estimating the value of S and β for stage 2. This was not possible as the product quantity was very low (∼30 × 10^{-9} mol). We, therefore, estimated the relative S-33 and S-34% composition of the product obtained in stage 2 using the following methodology.

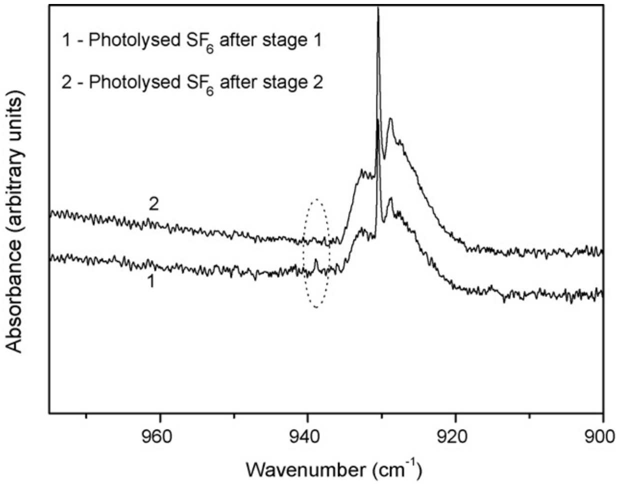

Fig. 6. IR spectra of photolysed SF_6 after stage 1 and stage 2 (irradiation at −78 °C for both stages). (1) Enriched SF_6 after stage 1 photolysis at −78 °C (^{32}S:^{33}S:^{34}S = ∼0:12:88). (2) Enriched SF_6 after stage 2 photolysis at −78 °C.

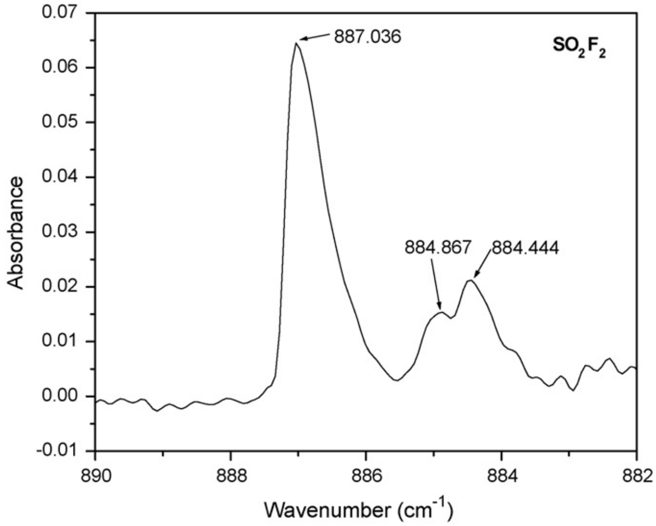

Fig. 7. Typical spectral details of enriched SO_2F_2 product (laser selectively tuned to $^{32}SF_6$ in stage 1).

The measured $d(^{33}SF_6)$ value for 39% decomposition after 900 pulses was 5 × 10^{-4}. There was no measurable decomposition in $^{34}SF_6$. Assuming a 1% decomposition for the same, $d(^{34}SF_6)$ was 1 × 10^{-5}. This resulted in a S value of 50 for stage 2. As the minor isotopic species, $^{33}SF_6$, was targeted, the product enrichment factor, $\beta_{\text{product}}(33/34)$, will be same as the dissociation selectivity S in stage 2:

$$\beta_{\text{product}}\left(\frac{33}{34}\right) = \frac{(^{33}SF_6/^{34}SF_6)_{\text{stage 2}}}{(^{33}SF_6/^{34}SF_6)_{\text{stage 1}}} = 50$$

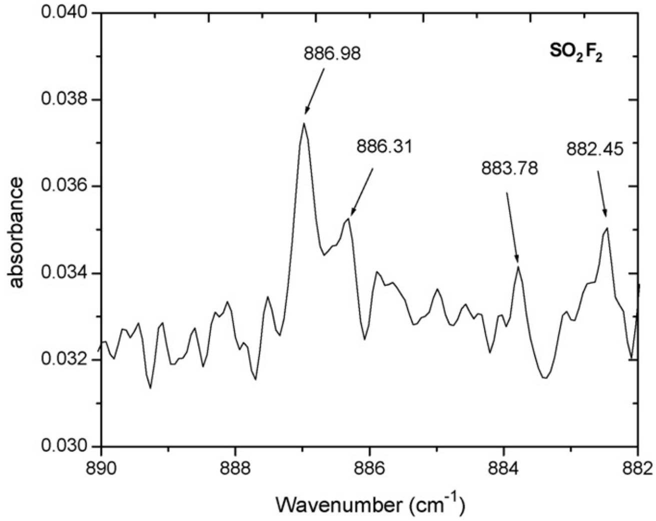

Fig. 8. Typical spectral details of enriched SO_2F_2 product (laser selectively tuned to $^{33}SF_6$ in stage 2).

Using the value for $(^{33}SF_6/^{34}SF_6)_{\text{stage 1}}$ obtained from our experimental results in stage 1, the relative % composition of ^{33}S:^{34}S in the product formed in stage 2 was estimated to be 92:8%.

Though we could not directly measure the individual isotopic composition in SO_2F_2, we have shown that by burning almost all the $^{32}SF_6$ in stage 1 and targeting $^{33}SF_6$ with good selectivity with respect to $^{34}SF_6$ in stage 2, it is possible to obtain a final product in stage 2 with a high S-33 content.

4. Conclusion

In summary, we have investigated the enrichment of S-33 isotopes using the IR laser chemistry of SF_6 by systematic variation of experimental parameters like, substrate pressure, temperature, scavenger, laser frequency and fluence. Adapting a novel two-stage scheme, high enrichment in S-33 has been realized by the appropriate choice of parameters and experimental conditions in successive stages. Further studies are needed to address issues like S-33 production rate under optimized conditions.

Acknowledgements

The authors would like to thank Drs. A.K. Ray and L.M. Gantayet, BARC for their keen interest and support of this work. They are also grateful to Dr. Werner Fuss for helpful suggestions and discussion. Mr. Naveen Kumar's assistance in recording the FTIR spectra is acknowledged.

References

[1] J. Sambrook, et al., Molecular Cloning, Cold Spring Harbor Laboratory Press, 1989.

[2] G.H. Keller, M.M. Mank, DNA Probe, Stockton Press, 1993.

[3] V.N. Bagratashvili, Yu.R. Kolomisky, V.S. Letokhov, E.A. Ryabov, V.Yu. Baranov, S.A. Kazakov, V.G. Nizjev, V.D. Pismenny, A.I. Starodubtsev, E.P. Velikhov, Appl. Phys. 14 (1977) 217.

[4] J.L. Lyman, S.D. Rockwood, S.M. Freund, J. Chem. Phys. 67 (1977) 4545.

[5] V.Yu. Baranov, E.P. Velikhov, S.A. Kazakov, Yu.R. Kolomisky, V.S. Letokhov, V.D. Pismenny, E.A. Ryabov, A.I. Starodubtsev, Sov. J. Quantum Electr. 9 (4) (1979) 486.

[6] V.Yu. Baranov, E.P. Velikhov, Yu.R. Kolomisky, V.S. Letokhov, V.G. Nigev, V.D. Pismenny, E.A. Ryabov, Sov. J. Quantum Electr. 9 (5) (1979) 621.

[7] S.T. Lin, S.M. Lee, A.M. Ronn, Chem. Phys. Lett. 53 (1973) 260.

[8] W. Fuss, T.P. Cotter, Appl. Phys. 12 (1977) 265.

[9] U. Del Bello, V. Churakov, W. Fuss, K.L. Kompa, B. Maurer, C. Schwab, L. Werner, Appl. Phys. B 42 (1987) 147.

[10] S.K. Sarkar, A. Nath, U.K. Chatterjee, J.P. Mittal, K.V.S. Rama Rao, Ind. J. Phys. B 54 (1980) 311.

[11] H. Brunet, M. Perez, J. Mol. Spectrosc. 29 (1969) 472.

[12] W. Fuss, W.E. Schmidt, Ber. Bunsenges. Phys. Chem. 83 (1979) 1148.

[13] Anju Batra, S.K. Sarkar, V. Parthasarathy, J. Photochem. Photobiol. A: Chem. 83 (1994) 193.

[14] P.H. Ma, K. Sugita, S. Arai, Appl. Phys. B 49 (1984) 503.

[15] W. Fuss, K. Kompa, Prog. Quantum Electr. 7 (1981) 117.

[16] T. Schimanouchi, J. Phys. Chem. Ref. Data 6 (1972) 993.